VALIDATION OF A FULLY-MIXED MODEL FOR SIMULATING GAS-FIRED WATER STORAGE TANKS

Weimin Wang, Ian Beausoleil-Morrison, Martin Thomas, Alex Ferguson

CANMET Energy Technology Center, Natural Resources Canada
580 Booth Street, Ottawa K1A 0E4

ABSTRACT

An ESP-r component model for gas-fired water storage tanks was developed within the context of the simulation for building-integrated cogeneration systems. Charged by the cogeneration unit with gas back-up, the tank can be used to satisfy both domestic hot water needs and space heating. Based on the fully-mixed water assumption, the model has three control volumes representing the water and casing, the combustion chamber, and the flue gas. The experimental data used in this validation study comes from nine groups of tests, covering four commercial water heaters and three different water drawing schedules. The validation is carried out via a plant network with two components: the water tank and a boundary condition. It is found that the model can predict the mean tank temperature well. However, the fully-mixed assumption may lead to an underestimation of energy consumption by 8-15%, depending on the water drawing schedule.

KEYWORDS

Water tanks, Computer simulation, Empirical validation, Thermal stratification

INTRODUCTION

There is growing interest in using a water storage tank to satisfy both space heating and domestic hot water needs for residential buildings. Such a combined system offers the potential advantages of part-load performance improvement and capital cost reduction (Weiss 2003). Since the water tank is usually charged by the energy from solar collectors or other components which may not work continuously, an auxilary heater is needed to maintain a set temperatere in the tank.

Modelling water storage tanks has been a research topic for many years. Many mathematical models, experiments, and simulation programs have been reported in the literature, especially in the field of solar water heating. Since the inlet temperature to solar collectors has substantial impact on the performance of solar thermal systems, most previous studies focus on modelling thermal stratification and the resulting temperature profiles in the water tank. The degree of stratification is affected by the following major factors (Shyu et al. 1989): thermal mixing and the forced convective flow due to water draws; the natural convective flow due to the heat loss to the surrounding and thermal diffusion from hot layers to cold layers. These factors are considered in available models with varying degrees of complexity. For example, two dimensional models are presented in (Cabelli 1977; Lightstone et al. 1989; Oliveski et al. 2003) to consider the impact of charging or discharging water on stratification. Shyu et al. (1989) investigated the effects of tank wall and insulation on thermal stratification. Zurigat et al. (1989) compared six one-dimensional models for stratified water storage tanks. Different mechanisms are employed in these one-dimensional models to consider thermal mixing at water inlets. While two-dimensional models are more powerful in accounting for different factors affecting stratification, they are computationally expensive and require detailed input data, which could render them unsuitable for use in building simulations. In TRNSYS, for example, all four models (Type 4, 35, 60 and 140) for water storage tanks follow the one-dimensional approach: the tank is divided into a number of isothermal layers and mass and energy balance equations are established for each layer. These four TRNSYS models have different features such as the number of inlets, outlets, immersed heat exchangers and auxiliary heaters, and the method to consider heat loss to the surrounding (Druck and Pauschinger 1997; Klein et al. 2004). Although the auxiliary heater can be heated by either electricity or gas, the TRNSYS models treat the gas heater simply as an electrical one with a flue.

The model examined in this paper was developed specifically for gas-fired water storage tanks. It was developed for use in modelling residential cogeneration systems, the performance of which is less sensitive than solar thermal systems to water inlet temperature. Therefore, stratification is not considered at the current stage for the sake of simplicity. The current paper examines the validity of this model. It studies the model's accuracy in predicting energy consumption and the difference between simulated tank temperature and the outlet temperature. The quantified deviation will be used as a reference in future performance assessment of cogeneration systems. This paper is organized as follows. The mathematical model is described next. Then, sections 3 and 4 give an introduction of the

experimental data and how the model input data are prepared based on the experimental data. The ESP-r simulation model is briefly presented in section 5. The simulation results are compared with the experimental data in section 6. Some concluding remarks are made finally.

GAS-FIRED WATER STORAGE TANK MODEL

In ESP-r (Clarke 2001), each plant component is represented by one or more discrete control volumes (nodes). For each node, the governing equations are established according to the principles of conservation for mass, energy and momentum. For the gas-fired water storage tank, the model was developed with three nodes (Figure 1): node 1 for the water and casing; node 2 for the combustion chamber; and node 3 for the flue. This three-node approach was used because it facilitates future expansion to incorporate explicit combustion modeling and the heat transfer processes between the flue and the water tank (Beausoleil-Morrison 2001). The energy balance equation for each node is described next.

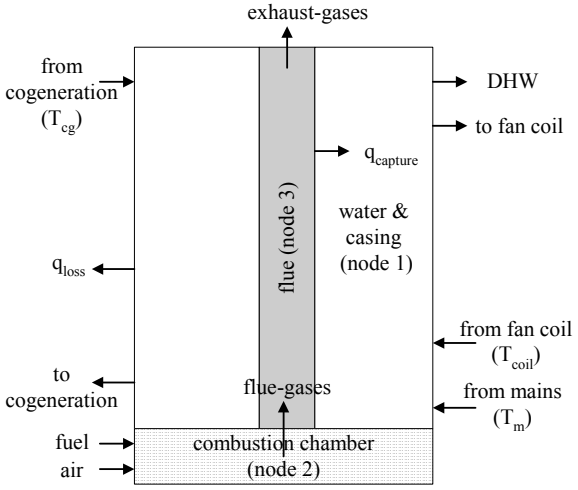

Figure 1 Three-node representation of gas-fired storage water tank

Energy balance for node 1

The water tank model was developed within the context of the simulation for building-integrated cogeneration systems. Charged by the cogeneration unit with gas back-up, the hot water can be supplied to the fan coil for space heating and various outlets for domestic hot water (DHW) needs. Based on the connection scheme in Figure 1, the energy balance for the water and casing (node 1) is given as:

$$(Mc_p)_1 \frac{\partial T_1}{\partial t} = q_{capture} - q_{loss} + (\dot{m}c_p)_{cg}(T_{cg} - T_1) + (\dot{m}c_p)_{coil}(T_r - T_1) + (\dot{m}c_p)_{DHW}(T_m - T_1) \quad (1)$$

where, the term on the left side represents the heat storage of the water tank; on the right side, $q_{capture}$ is the heat transferred to the water from the flue gases, q_{loss} is the skin heat loss from the tank casing, the 3rd to 5th terms represent the net energy flows from the cogeneration unit, the fan-coil for space heating, and the water mains for DHW make-up, respectively.

Since the heat transfer process between the flue and the water tank is not explicitly modeled in the current stage, the term $q_{capture}$ is simply derived from the the following equation:

$$q_{capture} = \mu \cdot q_{burner} \quad (2)$$

where, q_{burner} is the energy released by the fuel's combustion and μ is the overall efficiency of combustion and of the heat transfer between the flue and water. The value of μ is equal to the fraction of the energy released by the fuel's combustion that is transferred to the water. The overall efficiency is assumed to be constant in this model and given as a user input.

The skin heat loss from the water tank to its surrounding is calculated with

$$q_{loss} = (UA) \cdot (T_1 - T_{env}) \quad (3)$$

where, UA is heat loss coefficient, T_{env} is the temperature of environment.

Energy balance for nodes 2 and 3

The energy balance equations for node 2 and node 3 are given as:

$$(\dot{m}h)_{fuel} + (\dot{m}h)_{air} + q_{burner} = (\dot{m}h)_{flue-gases} \quad (4)$$

$$(\dot{m}h)_{flue-gases} = (\dot{m}h)_{exhaust-gases} + q_{capture} \quad (5)$$

In the above equations, the flow rate of fuel, air, and flue gases, and the enthalpy of the fuel and air streams entering the combustion chamber are calculated based on the molar fraction of fuel constituents, the excess air ratio, and the burner capacity. The linearization approach can be used to relate the enthalpy of flue gases and exhaust gases to the corresponding node temperature. The detailed description of these calculations can be found in (Beausoleil-Morrison 2001).

According to the chosen implicit/explicit scheme, equations 1, 4, and 5 are used to derive the energy balance matrix coefficients for the gas-fired water tank. These coefficients are then embedded into the integrated matrix for all the plant components of the HVAC system. The matrix equation is solved in ESP-r with a direct solution approach to obtain the three node temperatures. Since the equation set is

highly nonlinear, iteration is required to update and resolve the matrix until convergence is achieved.

EXPERIMENTAL DATA

Experimental data were gathered from a series of tests carried out at Natural Resources Canada. The purpose of these tests was to measure the energy consumption and efficiency of gas-fired water heaters.

Four different water heater models were used in the tests: model A is a power-vented water heater, which uses draft fans to push the exhaust gases away; models B and C are conventional water heaters, which use room air for combustion and natural draft for the exhaust; model D is a direct-vented water heater, which draws air from outside the building directly into the combustion chamber.

Three water draw schedules were used in the tests: the draw schedule specified in the standard CAN/CSA-P.3-04 (CSA 2004), the draw schedule used at the Canadian Center for Housing Technology (CCHT 2007), and a hypothetical draw schedule speculated by the tester. The CSA schedule has a total of six draws for a simulated day. Each draw starts at the beginning of the first six hours and has a volume about 40.6 L. The CCHT schedule has a total of eight draws per day. The corresponding volume and time for each of the eight draws are specified as 25 L/7:00, 11 L/8:00, 8 L/13:00, 27 L/18:00, 14 L/19:00, 19 L/20:00, 34 L/21:00, and 39 L/23:00. The hypothetical schedule has a draw every hour. Each draw starts at the 50th minute and has a volume of about 61 L.

All water heater models were tested following the CSA schedule while only model A was tested following the CCHT schedule and the hypothetical schedule. Table 1 gives an overview of all the tests covering different water heater models and water draw schedules.

Table 1: Overview of tests

HEATER MODEL	VENT TYPE	TEST	DRAW SCHEDULE
A	power-vented	A-1	CSA
		A-2	CSA
		A-3	CCHT
		A-4	CCHT
		A-5	hypothetical
B	conventional	B-1	CSA
		B-2	CSA
C	conventional	C-1	CSA
D	direct-vented	D-1	CSA

The experiment was set up according to the standard CAN/CSA-P.3-04 (CSA 2004). All tests start just after cut-out, which is the moment in time when the water heater thermostat has acted to reduce the fuel supply to the burner to its minimum (zero if no pilot power exists). Due to different purposes of the original tests, the CSA scheduled tests differ from the tests with the other two schedules in the following two aspects:

- The inlet water temperature. For the CSA scheduled tests, the water supply to the water heater inlet is maintained at a constant temperature of about 14 ºC. In contrast, for the tests with the CCHT and hypothetical schedules, the supply water is directly taken from the water mains and its temperature may vary between 5 and 10 ºC.
- The data measurement in terms of scope and frequency. For the CSA scheduled tests, the following data were measured every two seconds during the six water-drawing periods and ten seconds during the standby period: the concentration of O_2, CO, CO_2, and NO in the flue gas, the water inlet and outlet temperature, the water flow, the room temperature, the flue gas temperature, and the tank water temperature. In particular, the tank water temperatures were measured with six thermocouples equally distributed along the vertical line of the tank. Besides the above regular measurements, gas consumption was measured for all burner-on periods during the test. For the tests with the CCHT and hypothetical schedules, the measurements are limited to the water inlet and outlet temperature, the water flow, the room temperature, and the gas consumption. These measurements are recorded every twenty seconds.

CALIBRATING MODEL

The experimental data are used to "calibrate" the previously described model in order to establish the model inputs. The calibrated model inputs include the heat loss coefficient UA, the overall efficiency μ, the pilot power q_{pilot} , and the excess air ratio.

Since the tests originally aimed at determining the efficiency of gas-fired water heaters, the measured data can be conveniently employed to calculate the water heater's recovery efficiency, which is defined as "the ratio of the energy imparted to the water to the energy content of the fuel consumed by the burner during the period that the water temperature is raised from the inlet temperature to the final temperature, with the tank filled to capacity" (CSA 2004). The recovery efficiency is then used as the basis to calculate both UA and μ.

The recovery efficiency η of a gas-fired water heater is computed as (CSA 2004):

$$\eta = \frac{M_1 c_{p1}(T_{out} - T_{in}) + Mc_{p2}(T_{max,1} - T_0)}{Q_1} \quad (6)$$

where, M_1 is the mass of water withdrawn during the first draw, M is the mass of water in the tank, T_{out} and T_{in} are the average outlet and inlet temperature for the first draw, $T_{max,1}$ is the maximum mean tank temperature recorded after the first cut-out, T_0 is the mean tank temperature prior to the first draw, c_{p1} and c_{p2} are the specific heat of water respectively at $(T_{out} + T_{in})/2$ and $(T_{max} + T_0)/2$, Q_1 is the energy consumed in the first drawing period (from the start of the test to the first cut-out).

Considering that the heat loss coefficient UA is regarded as a constant in the model, it is better to derive its value that can mostly represent the water heater states in terms of the mean tank temperature and the burner status. Therefore, the calculation of UA is based on the standby period lasting from the time at which the maximum mean tank temperature is observed after the sixth draw to the end of the test. The UA is calculated as:

$$UA = \frac{q_{stby}}{T_{t,stby} - T_{a,stby}} = \frac{Q_{stby}\eta - Mc_p(T_{24} - T_{max,6})}{\tau_{stby} \cdot (T_{t,stby} - T_{a,stby})} \quad (7)$$

where, q_{stby} is the standby loss rate, Q_{stby} is the total energy consumption during the standby period, $T_{t,stby}$ and $T_{a,stby}$ are respectively the average water temperature and ambient temperature during the standby period, T_{24} is the mean water temperature at the end of the test, T_{su} is the maximum mean water temperature observed after the sixth draw, τ_{stdby} is the length of the standby period.

The overall efficiency (μ) used in the model does not take the same value as the recovery efficiency (η) calculated from Equation 6. This is because the heat loss to the surrounding is considered by η but not by μ. Therefore, the following equation is employed to calculate μ from η:

$$\mu = \eta + \frac{UA \cdot \tau_1 \cdot (T_{t,1} - T_{a,1})}{Q_1} \quad (8)$$

where, $T_{t,1}$ and $T_{a,1}$ are respectively the average water temperature and ambient temperature during the first drawing period, τ_1 is the length of the first drawing period.

It is observed that for the tested water heaters with permanent pilot, the burner is not activated during the standby period. Hence, the pilot power can be simply calculated as:

$$q_{pilot} = \frac{Q_{stby}}{\tau_{stby}} \quad (9)$$

The excess air ratio is calculated based on the O_2 concentration in flue gas, the molar fraction of fuel constituents, and the chemical reactions involved in fuel combustion. The details are not presented here due to space limitation.

With all the equations described in this section, the model input data for the CSA-scheduled tests are calculated and the results are given in Table 2. The model input data for the tests with the CCHT schedule (A-3 and A-4) and the hypothetical schedule (A-5) take the average of tests A-1 and A-2 because the tank temperature was not recorded. Table 2 also lists the rated burner-on capacity $q_{burner-on}$ and the calibrated tank volume.

ESP-R SIMULATIONS

Since this study aims to validate the tank model's prediction when subjected to external loads, a plant network is created with two components: a gas-fired water tank and a boundary condition. The boundary condition is used as the water flow source for the tank. With only one connection applicable in this study, the 3rd and the 4th items at the right side of equation 1 will vanish while for the existing 5th item, both the water flow rate and water inlet temperature are fed from a boundary condition file. This file has a one-minute frequency of data records; therefore, the original test data are processed in the following ways to obtain the required boundary conditions:

- The water flow rate in kg/s derives from the measured water flow in L for every minute. Since the water flow may not last for a whole minute, the derived flow rate may take different values during the water drawing periods. This difference has negligible impact on simulation results because each draw is short in time (about 4 minutes) and for each draw the total volume withdrawn from the tank keeps the same value as that for the experiment.
- The water inlet temperature T_m is averaged only for those data records with non-zero water flow, instead of all data records within a minute. This treatment is necessary because a water draw may not last for a whole minute.

In this ESP-r simulation model, the gas-fired water tank uses a temperature-based control. The burner is fired if the tank temperature is less than the signal on setpoint temperature T_{set-on} or if it was on for the

previous time step and the tank temperature is less than the signal off setpoint temperature $T_{set-off}$. The well-mixed nature of the water tank model determines that the mean tank temperature needs to be used as the setpoints. Therefore, both T_{set-on} and $T_{set-off}$ are extracted from the experimental data by averaging the mean tank temperatures corresponding to the change of burner status from off to on or vice versa during a test.

The established ESP-r model assumes that the tank locates at a room with a constant temperature, which takes the average value of all measured room tempertatures for each test. This assumption is reasonable because the room temperature has only a small fluctuation of about 0.5 ºC.

COMPARISON OF MODEL PREDICTIONS TO EXPERIMENTAL DATA

After running the simulation, the results are compared with the experimental data. The comparison in this paper concentrates on the tank temperature and the energy consumption.

Figures 2 and 3 respectively show the change of tank temperature during the water-drawing periods and the standby period for test B-1. These two figures lead to the following observations:

- Generally, the predicted mean tank temperature complies well with the test data. One most significant temperature difference (about 1.4 ºC) occurs at the end of cut-out following the first draw (Figure 2). This difference is mainly due to the deviation of observed temperature setpoints for different on-off cycles. It is found that the mean tank temperature at the first cut-out is about 0.9 ºC lower than the $T_{set-off}$ value used in the model input.
- During the subsequent hour after each cut-out, the predicted tank temperature decreases faster than the test data (Figure 2). This is because thermal mixing and the residual heat transfer from the flue to the tank after the burner off are not considered in the model. In addition, because the thermal mixing due to water draws and the start-up characteristics of the burner are not considered in the model, the tank temperature increases right after the burner is fired while there is a time lag in the test. The time lag can explain the difference of about 1.5 ºC between the simulation and the test when the tank temperature begins to increase (Figure 2).
- In the standby period (Figure 3), the temperature vs. time curves for the simulation and the test are close and almost parallel with each other. This observation demonstrates that the heat loss to the surrounding is modeled correctly with its UA value.

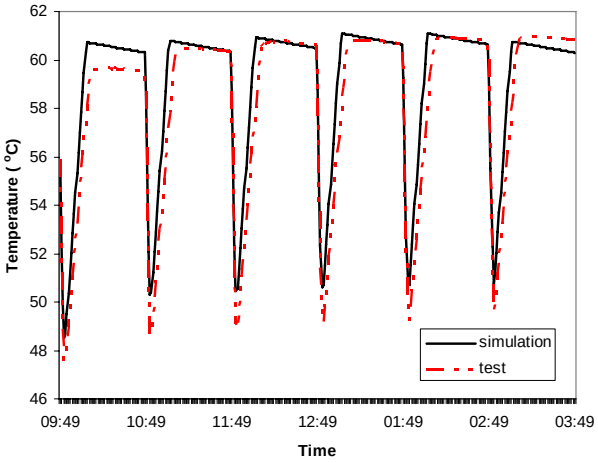

Figure 2 Comparison of tank temperature in the water drawing periods for test B-1

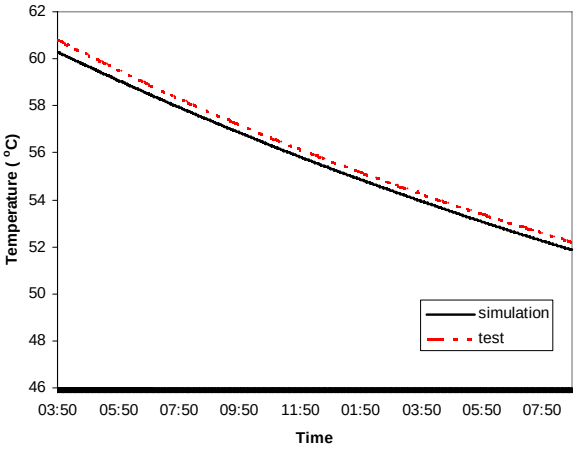

Figure 3 Comparison of tank temperature in the standby period for test B-1

Similar trends of tank temperature change with time are found for other CSA-scheduled tests except for the water heater model A. For example, Figure 4 shows the change of tank temperature for test A-1. In contrast to other tests, the burner is fired in the standby period because the model A has no pilot power. Moreover, there is an asynchronous change of burner status: the burner is fired earlier and shorter in the test than it in the simulation. This difference can be explained via the temperature setpoints defined in this study. Recall that the setpoints are derived by averaging the mean tank temperatures corresponding to the change of burner status. Hence, the control used in the simulation is an approximation of the actual control, which depends on the thermostat located in between the 3rd and the 4th thermocouples. Meanwhile, the change of sensed

temperatures has different characteristics due to water draws and standby losses. As illustrated in Figure 5, the lower parts of the tank (e.g., T_4 and T_6) have much lower temperatures after the water drawing than they have in the standby period, while the upper parts of the tank (e.g., T_1 and T_3) have higher temperatures after the water drawing than they have in the standby. In other words, the tank is more stratified after the water drawing. The overall consequence is that in the standby period, the mean tank temperature is still higher than the derived value T_{set-on} (=50.11 ºC) when the burner is fired in the test while it is still lower than $T_{set-off}$ (=58.46 ºC) when the burner is off.

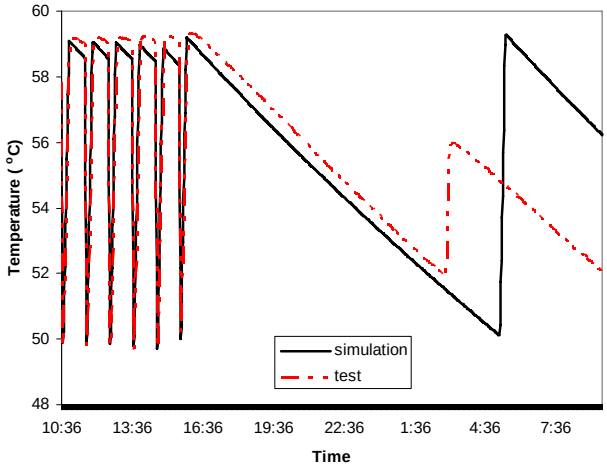

Figure 4 Comparison of tank temperature over the whole test period for test A-1

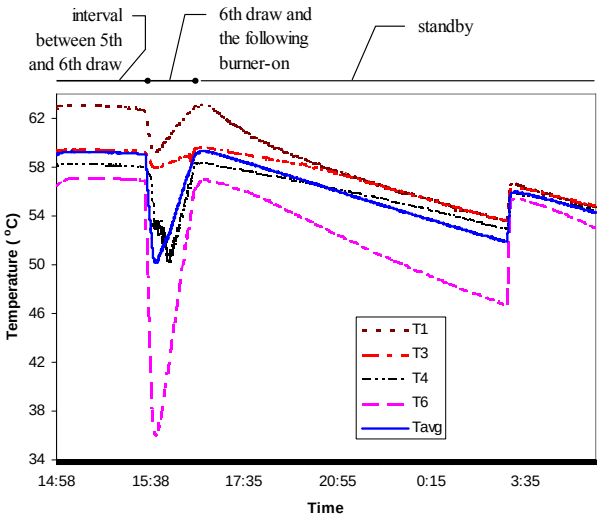

Figure 5: Measured temperatures at different levels and the mean tank temperature for test A-1

The third column in Table 3 lists the predicted energy consumption for all cases. Compared with the experiment, the simulation model has about 8% underestimation for the two CCHT scheduled tests (A-3 and A-4). The degree of underestimation is as large as about 15% for all other tests with the CSA schedule and the hypothetical schedule. The underestimation comes from the assumption of well-mixed water in the tank. Under this assumption, the energy delivery due to water flow is calculated as $(c_p\dot{m})_{DHW}(T_m - T_1)$, instead of $(c_p\dot{m})_{DHW}(T_m - T_{out})$. However, due to stratification, the mean tank temperature T_1 differs from the outlet temperature T_{out}. For example, Figure 6 shows their difference for the six water draws in test B-1. This figure demonstrates that T_1 may be more than 10 ºC lower than T_{out}. To examine the impact of using different temperatures T_1 and T_{out} on energy consumption, the delivered energy is calculated in the above two ways for each time step. Then, the delivered energy is integrated together for all time steps and the results are given in Table 4. This table demonstrates that the temperature difference between T_1 and T_{out} causes about 65-95% of the underestimated energy consumption. The rest of underestimation may be due to other factors such as the inaccuracy of experimental measurements and the simulation model inputs.

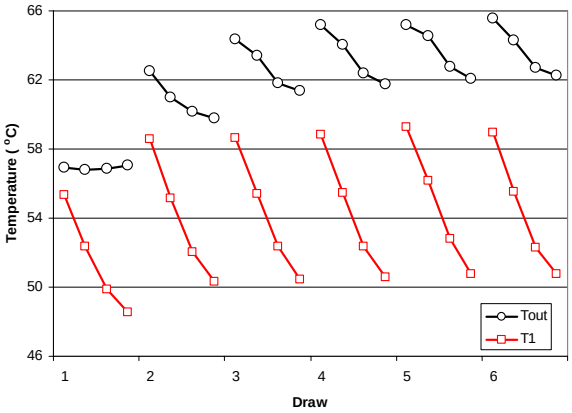

Figure 6 Comparison of outlet temperature T_{out} and mean temperature T_1 over the six draws in test B-1

The improved accuracy of predicted energy consumption using the outlet temperature T_{out} motivates the idea of representing the items of delivered energy from the tank connections in Equation 1 directly as the energy flow. For example, the third item and the fourth item can be replaced with the useable heat generation rate of the cogeneration unit and the heating load of the space, respectively. Thus, the modified equation 1 takes the following form for this study:

$$(Mc_p)_1 \frac{\partial T_1}{\partial t} = q_{capture} - q_{loss} + \sum q_{delivered} = q_{capture} - q_{loss} + (\dot{m}c_p)_{DHW}(T_m - T_{out}) \quad (10)$$

The T_{out} values are fed into the model via the boundary condition file and they are obtained from the experimental data through the same processing procedure as those for the item T_m . Based on Equation 10, the simulation model is rerun for each case and the results are presented in the rightmost column of Table 3. Because the impact of stratification on energy consumption has decreased significantly in Equation 10, the degree of underestimation reduces to less 6%. For some cases such as A-3, B-1 and B-2, there is negligible deviation between the simulation and test in terms of energy consumption.

CONCLUSIONS

A model for simulating gas-fired water storage tanks is presented in this paper. This model assumes that the tank water is well-mixed. The model's accuracy in predicting tank temperature and energy consumption is compared with nine groups of experimental data for commercial water heaters. The comparison leads to the following conclusions:

- The predicted mean tank temperature generally complies well with the test data. The major source of predication error comes from the temperature setpoints.
- The predicted mean temperature is about 4-12 ºC lower than the outlet temperature for most draws.
- Because of the fully-mixed assumption, the model underestimates energy consumption. The degree of underestimation depends on the water draw schedules: 8% of underestimation is found for the schedule imitating a normal house in Canada and about 15% of underestimation found for frequent, large volume water draws. The difference of outlet temperature and mean temperature is the main reason of underestimation. The error of predicted energy consumption can be reduced to less 6% by directly using the energy flow to establish the energy balance equation for node 1.

Major future work lies in two aspects: the consideration of stratification and the explicit modeling of combustion and flue-to-water heater transfer.

NOMENCLATURE

C_p	specific heat (J/kg-K)
h	enthalpy (J/kg)
M	mass (kg)
$\dot{m}$	mass flow rate (kg/s)
q	heat flow rate (W)
Q	energy (J)
T	temperature (K)
UA	heat loss coefficient (W/K)
t, τ	time (s)
η	recovery efficiency of water heater
μ	overall efficiency of burner

REFERENCES

Beausoleil-Morrison I. 2001. "Design of fuel cell component model for FCT project", Internal Report for CANMET Energy Technology Center in Ottawa, Natural Resources Canada, 16 pages.

Cabelli A. 1977. "Storage tanks-A numerical experiment", Solar Energy. 19:45-54.

CCHT. 2007. http://www.ccht-cctr.gc.ca, accessed in February, 2007.

Clarke JA. 2001. Energy Simulation in Building Design, 2nd edition. Oxford: Butterworth-Heinemann.

CSA. 2004. National Standard of Canada CAN/CSA-P.3-04. Testing Method for Measuring Energy Consumption and Determining Efficiencies of Gas-fired Water Heaters. Canadian Standards Association.

Druck F, and Pauschinger T. 1997. Multiport Store: model for TRNSYS Type 140. University of Stuttgart (Germany), 25 pages.

Klein SA, et al. 2004 TRNSYS, version 16. Solar Energy Laboratory, University of Wisconsin.

Lightstone MF, Raithby GD, and Hollands KGT. 1989. "Numerical simulation of the charging of liquid storage tanks: comparison with experiment", ASME Journal of Solar Energy Engineering. 111(3): 225-231.

Oliveski RC, Krenzinger A, and Vielmo HA. 2003. "Comparison between models for the simulation of hot water storage tanks", Solar Energy. 75(2): 121-134.

Shyu RJ, Lin JY, and Fang LJ. 1989. "Thermal analysis of stratified storage tanks", ASME Journal of Solar Energy Engineering. 111: 54-61.

Weiss W. (Editor). 2003. Solar heating systems for houses: a design handbook for solar combisystems. London : James & James.

Zurigat YH, Maloney KJ, and Ghajar AJ. 1989. "A comparison study of one-dimensional models for stratified thermal storage tanks", ASME Journal of Solar Energy Engineering. 111(3): 204-210.

Table 2: Technical parameters and model inputs for CSA-scheduled tests

TEST	η	UA (W/K)	μ	q_{pilot} (W)	$q_{burner-on}$ (kW)	VOLUME (L)
A-1	0.780	4.233	0.808	0	10.55	183.0
A-2	0.780	4.341	0.805	0	10.55	183.0
B-1	0.747	4.640	0.773	103	11.13	145.8
B-2	0.751	4.600	0.777	103	11.13	145.8
C-1	0.758	3.758	0.788	100	11.13	145.8
D-1	0.760	4.600	0.800	125	12.31	182.4

Table 3: Comparison of energy consumption between experiment and simulation based on different energy balance equations on node 1

TEST	MEASUREMENT (KJ)	BASED ON EQUATION 1		BASED ON EQUATION 10	
		PREDICTION 1 (KJ)	DEVIATION 1 (%)	PREDICTION 2 (KJ)	DEVIATION 2 (%)
A-1*	62457	53160	14.9	61390	1.7
A-2*	62383	52530	15.8	61390	1.6
A-3	61415	57590	6.2	60760	1.1
A-4	63834	58230	8.8	60760	4.8
A-5	404417	343020	15.2	380360	6.0
B-1	76074	65440	14.0	76030	0.1
B-2	75980	65440	13.9	75370	0.8
C-1	74884	62560	16.5	70510	5.9
D-1	78536	67360	14.2	75400	4.0

*Note: the energy consumed in the standby period is not accounted because of the serious asynchronous change of burner status as shown in Figure 4.

Table 4: Comparison of delivered energy using different temperatures and its impact on simulation results

TEST [1]	DELIVERED ENERGY 1 (KJ) [2]	DELIVERED ENERGY 2 (KJ) [3]	RESULTED DIFF. IN GAS ENERGY (KJ) [4]	SIMULATION DEVIATION (KJ) [5]#	ACCOUNTABLE DEVIATION (%) [6]
	$\sum \lvert c\dot{m}(T_m - T_{out}) \rvert$	$\sum \lvert c\dot{m}(T_m - T_1) \rvert$	$([2]-[3])/\eta$	measurement – prediction 1	
A-1	46260	39470	8705	9297	94
A-2	46440	39420	9000	9853	91
A-3	36250	34020	2859	3825	75
A-4	37220	34110	3987	5604	71
A-5	292760	262300	39051	61397	64
B-1	47520	39740	10415	10634	98
B-2	47470	39830	10173	10540	97
C-1	45770	39620	8113	12324	66
D-1	47580	41140	8474	11176	76

#Note: the values in column [5] are calculated as the difference of energy consumption between measurement and the simulation based on equation 1, the values of which are from Table 3.